How to cite: *Angew. Chem. Int. Ed.* **2023**, *62*, e202311721
doi.org/10.1002/anie.202311721

Metal Hydrides | Hot Paper

Accessing Ta/Cu Architectures via Metal-Metal Salt Metatheses: Heterobimetallic C–H Bond Activation Affords μ-Hydrides

*Michela L. Maiola and Joshua A. Buss**

Abstract: We employ a metal-metal salt metathesis strategy to access low-valent tantalum-copper heterometallic architectures (Ta–μ_2-H_2–Cu and Ta–μ_3-H_2–Cu_3) that emulate structural elements proposed for surface alloyed nanomaterials. Whereas cluster assembly with carbonylmetalates is well precedented, the use of the corresponding polyarene transition metal anions is underexplored, despite recognition of these highly reactive fragments as storable sources of atomic M^{n-}. Our application of this strategy provides structurally unique early-late bimetallic species. These complexes incorporate bridging hydride ligands during their syntheses, the origin of which is elucidated via detailed isotopic labelling studies. Modification of ancillary ligand sterics and electronics alters the mechanism of bimetallic assembly; a trinuclear complex resulting from dinuclear C–H activation is demonstrated as an intermediate *en route* to formation of the bimetallic. Further validating the promise of this rational, bottom-up approach, a unique tetranuclear species was synthesized, featuring a Ta centre bearing three Ta–Cu interactions.

Alloyed nanomaterials are a focal point of catalyst development in contemporary materials science due to the diversity of morphologies and the synergistic effects accessible when combining disparate metals.[1] Moreover, nanoalloyed catalysts offer significant cost benefits as the more precious component often emulates, or surpasses, its bulk reactivity as a diluent in a less-expensive host.[2] An underexplored class of nanoalloys feature early-late transition metal pairings,[3] which, as a result of the distinct metallic components, include polar interactions that demonstrate heightened reactivity toward small molecule activation.[3a,4] However, as the compositional complexity of the catalyst increases—particle size, metal identity, metal ratio, and mixing pattern—so too do the mechanistic possibilities, limiting fundamental studies of bond activation processes and leaving catalyst development empirically driven.[5]

Reactivity at surfaces commonly occurs at defect sites comprised of a handful of coordinatively unsaturated metals.[6] In this way, small molecular clusters can emulate features of these active sites, serving as structural models, functional mimics, or both (Figure 1A).[7] This "cluster-surface analogy"[7b,8] was initially proposed in the 1970s, but the structural fidelity and surface-likeness of the molecular compounds was limited by a lack of rational synthetic methods.[9] Cluster complex synthesis has been described as

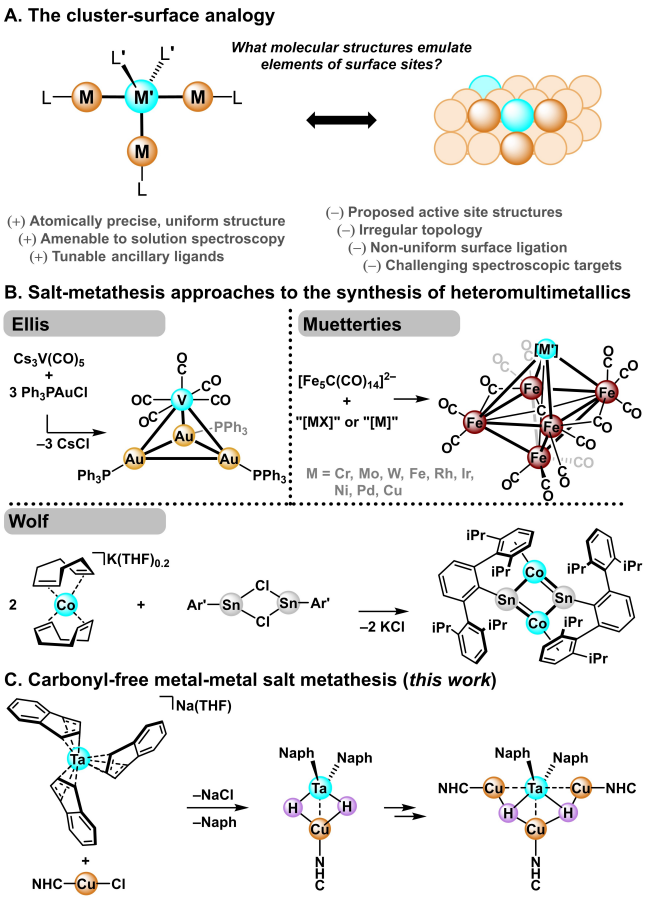


Figure 1. Atomically precise homogeneous metal clusters can inform structure/activity relationships at heterogeneous active sites (A) but the rational synthesis of molecular clusters remains a challenge. The metal-metal salt metathesis is a proven method in multimetallic complex synthesis (B), yet remains underexplored from precursors devoid of carbonyl ligands (C).

[*] M. L. Maiola, Prof. J. A. Buss
Willard Henry Dow Laboratory
Department of Chemistry, University of Michigan
930 N. University Avenue, Ann Arbor, MI 48109 (USA)
E-mail: jbuss@umich.edu

© 2023 The Authors. Angewandte Chemie International Edition published by Wiley-VCH GmbH. This is an open access article under the terms of the Creative Commons Attribution Non-Commercial NoDerivs License, which permits use and distribution in any medium, provided the original work is properly cited, the use is non-commercial and no modifications or adaptations are made.

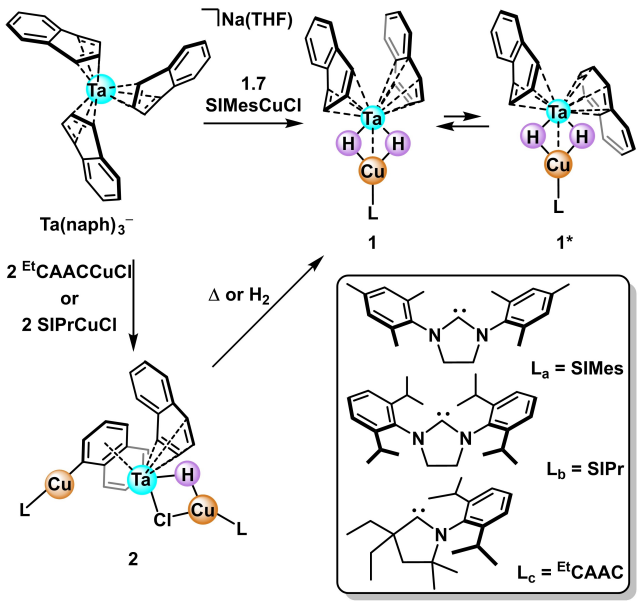
© 2023 The Authors. Angewandte Chemie International Edition published by Wiley-VCH GmbH

"something of a black art"[10] and has largely relied on self-assembly, particularly when targeting heteromultimetallics.[9a,10–11] To date, well-defined, bottom-up synthetic approaches for the construction of low oxidation state, metal-metal bonded clusters remain scarce.[11b,c,12] New methodologies for mixed-metal cluster syntheses are needed to access more accurate models of intricate metallic surface topologies.

A potentially versatile solution is the metal-metal salt metathesis—a reaction between anionic and cationic metal fragments. This approach allows for the selective construction of metal-metal bonds both from monometallic building blocks and in pre-formed clusters (Figure 1B).[10–11,13] More recently, this strategy has been leveraged to rationally access bi- and multi-metallic complexes with a wide array of structural diversity.[14] However, most examples have focused on carbonyl decorated precursors that can demonstrate attenuated reactivity and are often recalcitrant to ligand substitution following cluster assembly.[13a,15] Wolf and co-workers realized main-group/transition metal bond construction using a cyclooctadiene (COD) stabilized cobaltate synthon,[16] a promising precedent demonstrating dissociation of the COD ligand during the reaction sequence (Figure 1B).[16b] We hypothesized that a metathesis protocol employing homoleptic arene-supported metalates[17] could provide controlled synthetic access to unprecedented surface-like clusters and ultimately elucidate structure-function relationships in nanoalloyed catalysts.

Herein, we disclose the assembly of unusual tantalum/copper multimetallic constructs accessed through a CO-free metal-metal salt metathesis (Figure 1C). Detailed isotopic labelling studies shed light on unexpected cooperative C–H activation that occurs *en route* to bimetallic products. These species serve as rational precursors for higher nuclearity cluster preparation, facilitating the synthesis of a highly-reduced tetranuclear tricopper tantalum complex. The success of this approach validates, for the first time, the use of arene-stabilized anionic synthons in the predictable preparation of low-valent transition metal cluster compounds absent chelating or pre-templating supports. These should ultimately serve as robust and modular models for nanoalloy catalyst active sites.

To interrogate the assembly of clusters via super-reduced precursor addition, we explored reactions between Ellis' tris(naphthalene) tantalate ($[\mathbf{Ta(naph)_3}]^-$)[18] and carbene copper chlorides (Scheme 1).[19] In related salt metatheses with $CpM(CO)_2$ fragments, N-heterocyclic carbene supported coinage metals have demonstrated preferential stability relative to their phosphine analogs.[14h,20] This property, in combination with the thermal stability and diffuse orbitals of the tantalum monoanion, was anticipated to engender successful metal-metal bond construction. Addition of SIMesCuCl to a dimethoxyethane solution of $[\mathbf{Ta(naph)_3}]^-$ resulted in the gradual formation of a bright orange species. The resonances of the bound naphthyl ligands provide a responsive spectroscopic handle, informing compound symmetry and speciation.[21] ^{1}H nuclear magnetic resonance (NMR) spectroscopy showed the maintenance of four naphthyl signals, in a relative 2:1 integration with the



Scheme 1. Synthetic pathway to mixed Cu/Ta di- and trinuclear complexes preceding from an arene-supported metalate via metal-metal salt metathesis.

SIMes ancilliary ligand. The resonances for the tantalum-bound ring shift significantly downfield from the tantalate starting material ($\delta_{THF} = 4.44$ & 3.88 vs. 3.78 & 2.81, for [$H_{1,2}$] & [$H_{3,4}$], respectively),[22] consistent with diminished δ-back donation into the naphthyl π-system.[18] Additionally, the ^{1}H NMR spectrum evidenced an unexpected high field signal at −7.51 ppm (tetrahydrofuran-d_8 (THF-d_8); relative integration of two), suggesting the presence of hydride ligands. Taken together, these data suggested a dinuclear composition with a bis(μ-hydride) heterobimetallic diamond core (**1a**).

Single-crystal X-ray diffraction (SCXRD) analysis confirmed the formulation of **1a** (Figure 2).[23] The structure features two naphthalene rings with distinct hapticities, demonstrating both a more buckled η^4 (∠137.7°) and a more planar η^6 (∠156.6°) tantalum-arene interaction. The metrical parameters of the former closely resemble those of the tantalate starting material,[18] but both are consistent with the lessened back-bonding inferred spectroscopically, demonstrating diminished disruption of aromaticity in the Ta-bound rings. Despite apparent asymmetry in the solid-state, the naphthyl ligand coordination mode is fluxional in solution, wherein both rings are spectroscopically equivalent on the NMR timescale. The Ta–Cu distance, 2.654(1) Å, is close to the sum of the single-bond covalent radii of Ta and Cu (2.58 Å)[24] and is significantly shorter than other reported examples of Ta–(μ-H)$_2$–Cu motifs (*viz.* 2.84 Å).[25] In fact, **1a** has the shortest Ta–Cu distance reported to date.[26]

To determine the origin of the bridging hydride ligands, we first explored the role of solvent. Repeating the synthesis of **1a** in THF-d_8 resulted in partial deuteration of the bimetallic core (**1a**-d_1), as confirmed by ^{1}H and ^{2}H NMR spectroscopy (Figure S44). Utilizing $[\mathbf{Ta(naph}\text{-}d_8\mathbf{)_3}]^-$ in pro-

© 2023 The Authors. Angewandte Chemie International Edition published by Wiley-VCH GmbH

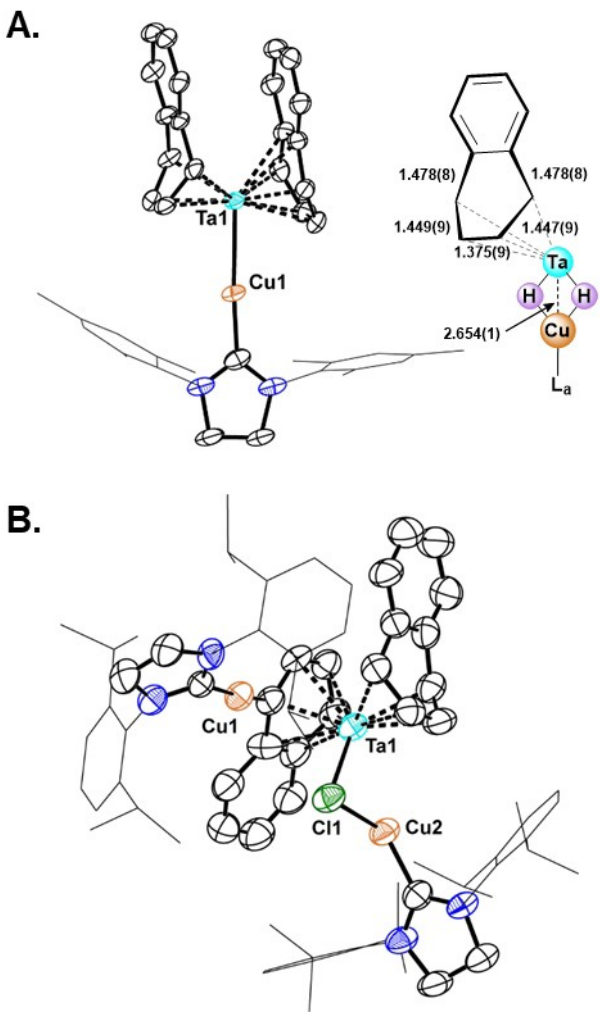


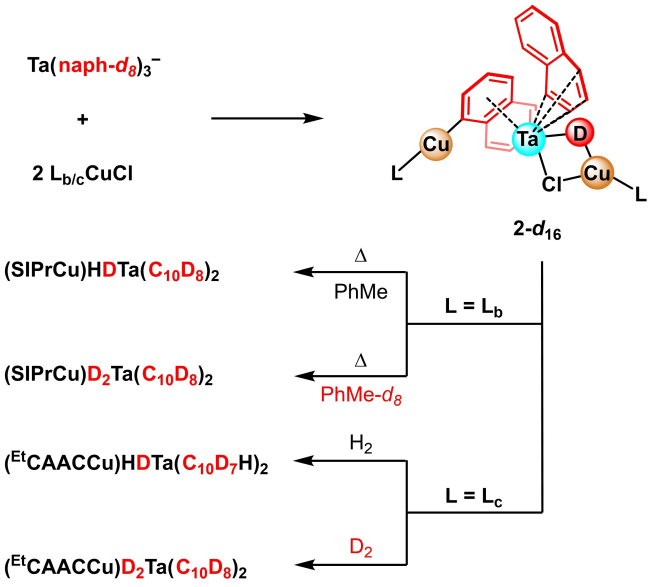
Figure 2. Single-crystal XRD structures (50% thermal anisotropic displacement ellipsoids) of **1a** (A) and **2b** (B). In each case, hydrogen atoms are omitted for clarity. Bond metrics (in Å) are provided for both the Ta–Cu bond and η^4-naphthyl C–C bonds in **1a**.

teo tetrahydrofuran (THF) failed to afford any deuterides in **1a**; however, the perdeuterated bimetallic was generated when both naphthalene and solvent were isotopically labeled. These results are consistent with one hydride originating from a homolytically weak solvent C–H bond. The source of the second hydride involves a naphthyl C–H bond activation event, presumably with simultaneous H/D exchange.

Further insight was gleaned by altering the identity of the copper synthon's carbene ligand. Reaction of **[Ta(naph)$_3$]$^-$** with sterically more encumbering SIPr (**L$_b$**, Scheme 1),[19b] led to the formation of a C_1 symmetric species with fifteen upfield shifted naphthyl signals (δ = 6.7–2.7 ppm; Figure S16) and a hydride resonance (δ = −4.73) in the ^{1}H NMR spectrum. The ^{1}H/^{13}C heteronuclear single quantum coherence spectrum identified five naphthyl ^{13}C resonances lacking ^{1}H cross-peaks, suggesting one naphthyl C–H bond as the source of the hydride ligand. SCXRD provided a decisive structural assignment.[23] The tantalum center retains two arene ligands, with the same η^4/η^6 hapticities observed in **1a** (albeit in a staggered orientation), but one ring concomitantly features a Cu–C sigma bond (1.896 (7) Å). The Ta coordination sphere is completed by a μ-Cl ligand and a SIPrCu fragment (Ta–Cu = 2.861(1) Å). The spectroscopically identified hydride ligand was not discernable in the Fourier map.

Considering the low-valent nature of these multimetallics, we anticipated that more π-acidic cyclic (alkyl)-(amino)carbene ligands (*viz.* Scheme 1, inset) might better stabilize critical reaction intermediates.[27] Interaction of **[Ta(naph)$_3$]$^-$** with ^{Et}CAACCuCl[19a] affords a highly soluble C_1 symmetric species that has evaded crystallographic characterization but bears spectroscopic features analogous to **2b**. Fifteen distinct naphthyl proton signals and a distinct hydride resonance (δ = −4.52) corroborate a heterotrinuclear composition, **2c**, with a naphthalene bridging between the copper (Cu–C σ-aryl) and tantalum (Ta η^6-arene) centers. Complexes **2b** and **2c** represent the products of a formal metal-metal salt metathesis, C–H activation, and LCuCl coordination sequence that may provide insight into the generation of the bimetallic species observed as the direct reaction product of the SIMes congener.

The deuteride complexes, **2b-*d*$_{16}$** and **2c-*d*$_{16}$**, were readily prepared from reactions of SIPrCuCl and ^{Et}CAACCuCl with **[Ta(naph-*d*$_8$)$_3$]$^-$**, respectively, further corroborating the presence (^{2}H NMR spectroscopy) and source (C–H activation of the Ta-bound naphthalene ring)[28] of the hydride ligand (Scheme 2). Prior experiments suggested the second hydride in **1a** originates from solvent (see above). To probe this further, **2b-*d*$_{16}$** was dissolved in toluene-*d*$_8$; no reactivity was observed at room temperature. Heating the reaction mixture to 110 °C for 10 hours yielded a new species with a ^{2}H NMR signal at −7.23 ppm. Repeating this experiment



Scheme 2. Synthetic pathway to access the deuterated SIPr and ^{Et}CAAC trinuclear complexes (**2a/b-d$_{16}$**), and subsequent reactions to probe hydride sources in **1b** and **1c**.

© 2023 The Authors. Angewandte Chemie International Edition published by Wiley-VCH GmbH

either in toluene or from **2b** gave the mixed isotopolog, and full characterization by NMR spectroscopy and SCXRD corroborated the generation of Ta/Cu bis(μ-hydride) complex, **1b**. Similar reactions with **2c**-d_{16} did not provide the desired dideuteride; however, addition of an atmosphere of D_2 to a benzene solution of **2c**–d_{16} at room temperature cleanly yielded **1c**-d_{18}. Crossover-type experiments confirm one hydride originates from H_2/D_2, and suggest that naphthalene C–H activation is reversible—a proton is incorporated into the ring when treating **2c**-d_{16} with H_2.[29] This was not observed for **2b**, but the interpretation of this result is complicated by both the generation of free naphthalene and the observation of naphthalene exchange under the more forcing reaction conditions.

Whereas these comparisons provide synthetic access to a conserved series of related bimetallics, the reaction mechanisms *en route* to each product are distinct. These reactivity manifolds appear sensitive to both carbene sterics (*i.e.* SIMes vs. SIPr) as well as electronics (*i.e.* SIMes vs. EtCAAC), though in each case, the data suggest one hydride results from bimetallic activation of a naphthyl ring. The solid-state structures of the bimetallic series—**1a**, **1b**, and **1c**—are similar; however, the hydride ligands for both **1b** and **1c** were discernable in the Fourier map (Figure S46 & S47).[23] One notable spectroscopic discrepancy between the complexes is the clear presence of a minor component in crystalline samples of **1c**. A second hydride resonance is observed at −5.33 ppm, along with additional signals corresponding to bound naphthyl peaks. Upon closer inspection, these same characteristic peaks were detected in the ^{1}H NMR spectra for **1a** and **1b**, albeit to a lesser extent (**1a**: *ca.* 15% [broad], **1b**: *ca.* 3%, **1c**: *ca.* 22%). Variable temperature NMR spectroscopy showed convergence of the distinct signatures of these two components upon heating, affording data consistent with an exchange process that is intermediate on the NMR timescale at 80 °C (Figure S32). We hypothesize that the minor species, based both on the number of peaks and their chemical shifts, is a C_s coordination isomer of **1** (demarcated **1***) resulting from a Ta-arene ring slip to a staggered Ta(naph)$_2$ confirmation (Scheme 1).[30] This process is more prevalent with sterically less congested complexes (**1a** and **1c**) than for the carbene ligand with bulkier substituents, as the C_s isomer directs one naphthyl ring toward the carbene *N*-aryl groups. In this way, the metal-arene interactions in these complexes prove quite dynamic, demonstrating both binding mode interconversion ($\eta^4 \leftrightarrow \eta^6$) and isomerization ($C_{2v} \leftrightarrow C_s$) in solution.

Recognizing that complex **1a** is formally more oxidized than **[Ta(naph)$_3$]**$^-$ and bears similarly accepting ligands (coinage metal LM^+ fragments are competent π-acceptors),[31] we targeted reduction chemistry as a means of rationally proliferating cluster nuclearity. Attempts to isolate reduction products have thus far been unfruitful; however, addition of potassium graphite (KC_8) to a thawing THF solution of **1a**, followed by *in situ* quenching with additional SIMesCuCl did result in productive salt metathesis chemistry (Figure 3A). A new hydride resonance (δ = −3.38) and dramatically upfield-shifted naphthyl protons (*cf.* δ = 1.43 & 1.79) were observed in the ^{1}H NMR spectrum of this new product, **3a**, consistent with a conserved, but more activated, (naph)$_2$Ta–(μ-H)$_2$–Cu core. Relative integration revealed a stoichiometry of three SIMes units per pair of naphthyl ligands, suggesting successful installation of two additional Cu carbene motifs. The ^{13}C{^{1}H} NMR spectrum exhibited both two low-field carbon resonances (δ = 157.27 & 146.96) in the region characteristic of η^4-napthalene species[18,21b] and signals consistent with three chemically distinct SIMes moieties, reflecting a descent in symmetry from the C_{2v} structure adopted by **1a**.

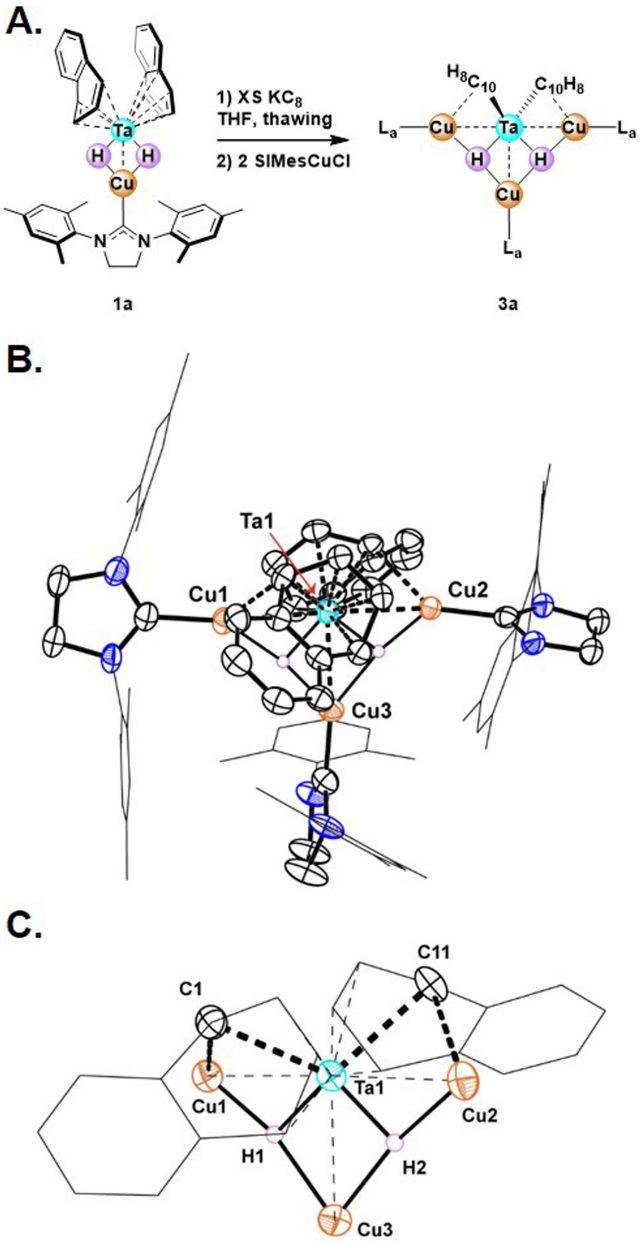


Figure 3. Synthetic pathway for mixed Cu/Ta cluster **3a** (A), single crystal XRD structure of the complete $TaCu_3$ complex (B), and a truncated depiction (side view) of the (naph)$_2$Ta–(μ-H$_2$)–Cu$_3$ core (C). Thermal anisotropic displacement ellipsoids are shown at the 50% probability level and non-hydride H-atoms are omitted for clarity. The hydride H-atoms were resolved in the Fourier map and refined freely.

© 2023 The Authors. Angewandte Chemie International Edition published by Wiley-VCH GmbH

A SCXRD study confirmed the $TaCu_3$ stoichiometry, revealing a T-shaped tetranuclear core for **3a** (Figure 3B&C).[23] The *trans*-SIMes units adopt orthogonal orientations, rationalizing the three ancillary ligand environments inferred spectroscopically. The hydrides were discernable in the Fourier map and bind in a μ_3-ηTa:ηCu:ηCu fashion. The Ta–Cu distances are similar (*ca.* 2.63 Å) and all three are slightly contracted relative to **1a**. The Ta–C_{naph} bonds display a long-short-short-long pattern reported previously for sterically encumbered group 4 metalate dianions,[32] reflecting crowding between the carbene mesitylene units and the naphthyl rings. Indeed, neither **3b** (SIPr) nor **3c** (^{Et}CAAC), both of which would have sterically larger diisopropylphenyl substituents, have been accessed to date. The most notable structural feature in **3a** is a short Cu–C_{naph} contact of $2.341_{(ave.)}$ Å between the flanking copper centers and the Ta-bound naphthyl groups. The C–C bonds around the ring are also asymmetric, with a statistically significant elongation on the side proximal to Cu (1.484 vs. 1.479 Å). Taken together, these solid-state metrics are most consistent with a μ_2-η^4Ta:η^1Cu binding mode for naphthalene. In this way, **3a** represents a rare example of an arene bridging ligand in a heteromultimetallic complex, and a particularly unusual instance of asymmetric M-arene-M′ bonding.[33]

To explore the nature of the bonding in the cores of **1** and **3**, we conducted density functional theory studies of truncated analogs (referred to henceforth as **1′** and **3′**, respectively) optimized at the PBE0/def2-TZVP–D3 level of theory.[34] For **1′**, Wiberg bond indices (WBI)[35] indicate Ta-centered M–H bonding, an electronic structure that was likewise inferred from orbital analysis (Figure 4A). The frontier orbitals display Ta–H bonding character with significant Cu–H antibonding contribution. Orbitals with in-phase 3c2e bonding overlap are all lower in energy, facilitated in part by symmetry-allowed p/d mixing on both metals. These considerations were bolstered by Quantum Theory of Atoms-In-Molecules (QTAIM) analysis,[36] which identifies bond critical points between the metal centers and the bridging hydride ligands.[37] The electron localization functions for the Ta–H bonds are nearly double that of the Cu–H bonds, corroborating Ta-centered hydrides. No bond critical point is identified between the metal centers, and both Natural Population Analysis (NPA) and the sub-unity Wiberg bond index suggest the M–M′ interaction has non-negligible ionic character ($q_{Ta} = -0.04$ and $q_{Cu} = 0.37$). This electronic structure is reminiscent, but much less polarized, than heterobimetallic Fe–Cu and Mo–Cu complexes that lack hydride bridges and have *bona fide* M–M bonds.[14h]

The bonding situation in **3′** is more complex (Figure 4B). Ta-centered hydrides (*cf.* HOMO-3) share bond paths with both adjacent copper centers (QTAIM) and similar bond indices were determined throughout the core (WBI). A notable distinction is seen in the QTAIM analysis, which identifies bond critical points between the metal centers, supporting increased metal-metal bonding character relative to **1′**. Additionally, the NPA charges—$q_{Ta} = -0.81$ and $q_{Cu} = 0.47_{(ave.)}$—reflect both the more reduced nature of the cluster and increased ionicity in the metal-metal bonding. The close Cu–C_{naph} contact is reproduced computationally, and, despite being adjacent to the naphthalene C–H bond, displays a Cu–C_{2p} backbonding interaction in agreement with the μ_2-η^4Ta:η^1Cu bonding prescribed above. Computed WBI for the bridging arene carbon (C_{naph}) indicate a dominant Ta-arene interaction ($0.53_{ave.}$) with non-negligible Cu-arene character ($0.14_{ave.}$).

In summary, we have successfully demonstrated the use of an arene-supported metallate, understudied sources of reactive M^{n-}, in a metal-metal salt metathesis protocol. This route provides a rational means of forging unusual, low-valent early-late heterobimetallic compounds. However, rather than mirroring the chemistry of carbonyl metallate analogs, the naphthalene ligated synthons undergo bimolecular C–H bond activation, generating bridging hydride ligands. Isotopic labeling studies and a comparison of sterically and electronically dissimilar carbene ancillary ligands establish the arene as the source of one hydride in the resultant Ta–(μ-H)$_2$–Cu core. Following formation of the initial bimetallic, subsequent reduction facilitates further *in situ* salt metatheses, in a sequence that rationally builds cluster nuclearity *en route* to a T-shaped heterotetranuclear cluster. Expanding this chemistry to new metal pairings, efforts to capitalize on naphthalene exchange,[21a] and exploration of the reactivity of these atypical multimetallic compounds are all underway in our laboratory.

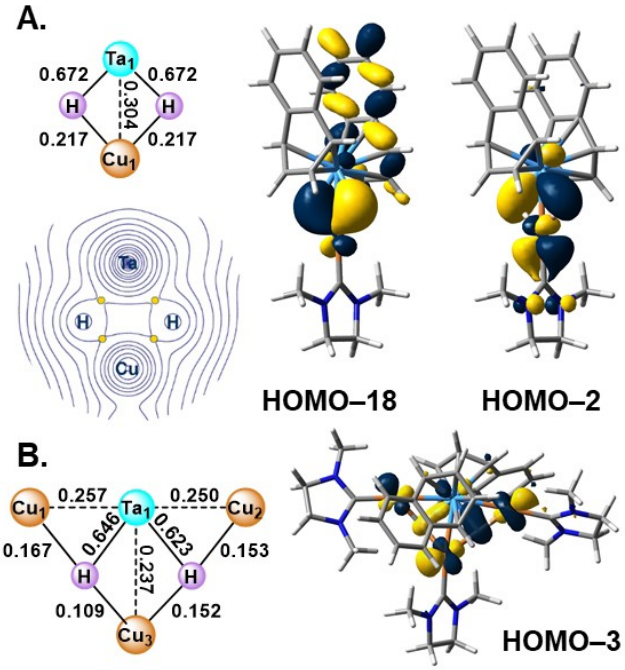


Figure 4. Select calculated Wiberg Bond Indices, QTAIM bond paths, and molecular orbitals for (naph)$_2$Ta–(μ-H$_2$)–Cu (A) and (naph)$_2$Ta–(μ-H$_2$)–Cu$_3$ (B) compounds. Isosurfaces are displayed at a 0.04 eA^{-3} level.

Acknowledgements

This work was supported by the University of Michigan and the NSF (Graduate Research Fellowship to M.L.M.; XRD

© 2023 The Authors. Angewandte Chemie International Edition published by Wiley-VCH GmbH

Instrumentation—CHE-0840456). We thank Dr. Eugenio Alvarado for NMR Spectroscopy expertise and Drs. Jeff Kampf and Fengrui Qu are gratefully acknowledged for assistance with SCXRD. Roy Wentz aided in the design and fabrication of custom glassware that made this work possible.

Conflict of Interest

The authors declare no conflict of interest.

Data Availability Statement

The data that support the findings of this study are available from the corresponding author upon reasonable request.

Keywords: Cluster Compounds · C–H Activation · Heterometallic Complexes · Hydrides · Metal-Metal Interactions

[1] a) K. Loza, M. Heggen, M. Epple, *Adv. Funct. Mater.* **2020**, *30*, 1909260; b) K.-H. Huynh, X.-H. Pham, J. Kim, S. H. Lee, H. Chang, W.-Y. Rho, B.-H. Jun, *Int. J. Mol. Sci.* **2020**, *21*, 5174; c) A. K. Singh, Q. Xu, *ChemCatChem* **2013**, *5*, 652–676; d) D. Wang, Y. Li, *Adv. Mater.* **2011**, *23*, 1044–1060.

[2] a) G. X. Pei, X. Y. Liu, X. Yang, L. Zhang, A. Wang, L. Li, H. Wang, X. Wang, T. Zhang, *ACS Catal.* **2017**, *7*, 1491–1500; b) F. R. Lucci, J. Liu, M. D. Marcinkowski, M. Yang, L. F. Allard, M. Flytzani-Stephanopoulos, E. C. H. Sykes, *Nat. Commun.* **2015**, *6*, 8550; c) X.-F. Yang, A. Wang, B. Qiao, J. Li, J. Liu, T. Zhang, *Acc. Chem. Res.* **2013**, *46*, 1740–1748; d) G. Kyriakou, M. B. Boucher, A. D. Jewell, E. A. Lewis, T. J. Lawton, A. E. Baber, H. L. Tierney, M. Flytzani-Stephanopoulos, E. C. H. Sykes, *Science* **2012**, *335*, 1209–1212; e) B. Qiao, A. Wang, X. Yang, L. F. Allard, Z. Jiang, Y. Cui, J. Liu, J. Li, T. Zhang, *Nat. Chem.* **2011**, *3*, 634–641.

[3] a) J. D. Lee, Z. Qi, A. C. Foucher, H. T. Ngan, K. Dennis, J. Cui, I. I. Sadykov, E. J. Crumlin, P. Sautet, E. A. Stach, C. M. Friend, R. J. Madix, J. Biener, *J. Am. Chem. Soc.* **2022**, *144*, 16778–16791; b) Y. Yao, Z. Huang, L. A. Hughes, J. Gao, T. Li, D. Morris, S. E. Zeltmann, B. H. Savitzky, C. Ophus, Y. Z. Finfrock, Q. Dong, M. Jiao, Y. Mao, M. Chi, P. Zhang, J. Li, A. M. Minor, R. Shahbazian-Yassar, L. Hu, *Matter* **2021**, *4*, 2340–2353; c) L. Xiong, K. L. More, T. He, *J. Power Sources* **2010**, *195*, 2570–2578; d) Z. Liu, J. E. Hu, Q. Wang, K. Gaskell, A. I. Frenkel, G. S. Jackson, B. Eichhorn, *J. Am. Chem. Soc.* **2009**, *131*, 6924–6925.

[4] a) J. Qin, Y. Zhang, D. Leng, F. Yin, *Sci. Rep.* **2020**, *10*, 14837; b) M. Escudero-Escribano, P. Malacrida, M. H. Hansen, U. G. Vej-Hansen, A. Velázquez-Palenzuela, V. Tripkovic, J. Schiøtz, J. Rossmeisl, I. E. L. Stephens, I. Chorkendorff, *Science* **2016**, *352*, 73–76; c) Q. Lu, G. S. Hutchings, W. Yu, Y. Zhou, R. V. Forest, R. Tao, J. Rosen, B. T. Yonemoto, Z. Cao, H. Zheng, J. Q. Xiao, F. Jiao, J. G. Chen, *Nat. Commun.* **2015**, *6*, 6567.

[5] C. Vogt, B. M. Weckhuysen, *Nat. Chem. Rev.* **2022**, *6*, 89–111.

[6] H. S. Taylor, *Proc. R. Soc. London* **1925**, *108*, 105–111.

[7] a) E. L. Muetterties, T. N. Rhodin, E. Band, C. F. Brucker, W. R. Pretzer, *Chem. Rev.* **1979**, *79*, 91–137; b) E. L. Muetterties, *Science* **1977**, *196*, 839.

[8] B. C. Gates, *Angew. Chem. Int. Ed.* **1993**, *32*, 228–229.

[9] a) G. L. Geoffroy, *Acc. Chem. Res.* **1980**, *13*, 469–476; There has been a renaissance of surface-informing molecular cluster chemistry in recent years. For molecular cluster chemistry relevant to chalcogenide and pnictogenide materials, see: b) B. S. Mitchell, A. Chirila, K. J. Anderton, W. Kaminsky, A. Velian, *Inorg. Chem.* **2023**, *62*, 10497–10503; c) B. S. Mitchell, A. Chirila, D. Y. Zhou, J. A. Kephart, A. Velian, *Inorg. Chem.* **2023**, *62*, 8789–8793; d) B. S. Mitchell, A. Chirila, J. A. Kephart, A. C. Boggiano, S. M. Krajewski, D. Rogers, W. Kaminsky, A. Velian, *J. Am. Chem. Soc.* **2022**, *144*, 18459–18469; e) J. A. Kephart, B. S. Mitchell, W. Kaminsky, A. Velian, *J. Am. Chem. Soc.* **2022**, *144*, 9206–9211; f) B. S. Mitchell, S. M. Krajewski, J. A. Kephart, D. Rogers, W. Kaminsky, A. Velian, *JACS Au* **2022**, *2*, 92–96; g) D. A. Reed, T. J. Hochuli, N. A. Gadjieva, S. He, R. A. Wiscons, A. K. Bartholomew, A. M. Champsaur, M. L. Steigerwald, X. Roy, C. Nuckolls, *J. Am. Chem. Soc.* **2022**, *144*, 306–313; h) C. M. Aikens, R. Jin, X. Roy, T. Tsukuda, *J. Chem. Phys.* **2022**, *156*, 170401; i) B. S. Mitchell, W. Kaminsky, A. Velian, *Inorg. Chem.* **2021**, *60*, 6135–6139; j) J. A. Kephart, A. C. Boggiano, W. Kaminsky, A. Velian, *Dalton Trans.* **2020**, *49*, 16464–16473; k) N. A. Gadjieva, A. M. Champsaur, M. L. Steigerwald, X. Roy, C. Nuckolls, *Eur. J. Inorg. Chem.* **2020**, 1245–1254; l) J. A. Kephart, B. S. Mitchell, A. Chirila, K. J. Anderton, D. Rogers, W. Kaminsky, A. Velian, *J. Am. Chem. Soc.* **2019**, *141*, 19605–19610; m) E. A. Doud, C. J. Butler, D. W. Paley, X. Roy, *Chem. Eur. J.* **2019**, *25*, 10840–10844; n) J. L. Stein, M. I. Steimle, M. W. Terban, A. Petrone, S. J. L. Billinge, X. Li, B. M. Cossairt, *Chem. Mater.* **2017**, *29*, 7984–7992; o) D. C. Gary, S. E. Flowers, W. Kaminsky, A. Petrone, X. Li, B. M. Cossairt, *J. Am. Chem. Soc.* **2016**, *138*, 1510–1513; For select recent examples of surface informing small molecule activation chemistry with mutimetallic complexes, see: p) L.-J. Liu, Z.-Y. Wang, Z.-Y. Wang, R. Wang, S.-Q. Zang, T. C. W. Mak, *Angew. Chem. Int. Ed.* **2022**, *61*, e202205626; q) S. Zhang, P. Cui, T. Liu, Q. Wang, T. J. Longo, L. M. Thierer, B. C. Manor, M. R. Gau, P. J. Carroll, G. C. Papaefthymiou, N. C. Tomson, *Angew. Chem. Int. Ed.* **2020**, *59*, 15215–15219; r) A. Z. Spentzos, M. R. Gau, P. J. Carroll, N. C. Tomson, *Chem. Commun.* **2020**, *56*, 9675–9678; s) T. Liu, M. R. Gau, N. C. Tomson, *J. Am. Chem. Soc.* **2020**, *142*, 8142–8146; t) M. M. Shoshani, R. Beck, X. Wang, M. J. McLaughlin, S. A. Johnson, *Inorg. Chem.* **2018**, *57*, 2438–2446; u) M. M. Shoshani, J. Liu, S. A. Johnson, *Organometallics* **2018**, *37*, 116–126; v) M. M. Shoshani, V. Semeniuchenko, S. A. Johnson, *Chem. Eur. J.* **2018**, *24*, 14282–14289; w) M. M. Shoshani, S. A. Johnson, *Nat. Chem.* **2017**, *9*, 1282–1285; For select recent examples of atomically precise metal-oxide cluster science, see: x) K. R. Proe, E. Schreiber, E. M. Matson, *Acc. Chem. Res.* **2023**, *56*, 1602–1612; y) M. Dagar, E. Schreiber, S. E. Cooney, E. M. Matson, *Inorg. Chem.* **2023**, *62*, 1763–1765; z) T. J. Barnes, J. Payne, S. D. Pike, *Chem. Commun.* **2023**, *59*, 59–62; aa) S. E. Brown, I. Mantaloufa, R. T. Andrews, T. J. Barnes, M. R. Lees, F. De Proft, A. V. Cunha, S. D. Pike, *Chem. Sci.* **2023**, *14*, 675–683; bb) R. L. Meyer, P. Miró, W. W. Brennessel, E. M. Matson, *Inorg. Chem.* **2021**, *60*, 13833–13843; cc) B. E. Petel, E. M. Matson, *Chem. Commun.* **2020**, *56*, 13477–13490; dd) A. H. M. Leung, A. García-Trenco, A. Phanopoulos, A. Regoutz, M. E. Schuster, S. D. Pike, M. S. P. Shaffer, C. K. Williams, *J. Mater. Chem.* **2020**, *8*, 11282–11291; ee) H. Lu, R. B. Jethwa, K. J. Jenkinson, A. E. H. Wheatley, H. Hao, D. S. Wright, S. D. Pike, *Dalton Trans.* **2019**, *48*, 4555–4564.

[10] G. L. Geoffroy, in *Stud. Surf. Sci. Catal, Vol. 29* (Eds.: B. C. Gates, L. Guczi, H. Knozinger), Elsevier, Amsterdam, **1986**, pp. 1–19.

[11] a) W. L. Gladfelter, G. L. Geoffroy, in *Adv. Organomet. Chem, Vol. 18* (Eds.: F. G. A. Stone, R. West), Academic Press, San

© 2023 The Authors. Angewandte Chemie International Edition published by Wiley-VCH GmbH

Diego, **1980**, pp. 207–273; b) E. V. Eames, R. Hernández Sánchez, T. A. Betley, *Inorg. Chem.* **2013**, *52*, 5006–5012; c) T. M. Powers, N. X. Gu, A. R. Fout, A. M. Baldwin, R. Hernández Sánchez, D. M. Alfonso, Y.-S. Chen, S.-L. Zheng, T. A. Betley, *J. Am. Chem. Soc.* **2013**, *135*, 14448–14458.

[12] a) A. W. Beamer, J. A. Buss, *J. Am. Chem. Soc.* **2023**, *145*, 12911–12919; b) M. K. Osei, S. Mirzaei, X. Bogetti, E. Castro, M. A. Rahman, S. Saxena, R. Hernández Sánchez, *Angew. Chem. Int. Ed.* **2022**, *61*, e202209529; c) M. C. Eaton, V. J. Catalano, J. Shearer, L. J. Murray, *J. Am. Chem. Soc.* **2021**, *143*, 5649–5653; d) J. L. Peltier, M. Soleilhavoup, D. Martin, R. Jazzar, G. Bertrand, *J. Am. Chem. Soc.* **2020**, *142*, 16479–16485; e) L. Jin, D. S. Weinberger, M. Melaimi, C. E. Moore, A. L. Rheingold, G. Bertrand, *Angew. Chem. Int. Ed.* **2014**, *53*, 9059–9063; f) T. J. Robilotto, J. Bacsa, T. G. Gray, J. P. Sadighi, *Angew. Chem. Int. Ed.* **2012**, *51*, 12077–12080; g) A. R. Fout, D. J. Xiao, Q. Zhao, T. D. Harris, E. R. King, E. V. Eames, S.-L. Zheng, T. A. Betley, *Inorg. Chem.* **2012**, *51*, 10290–10299; h) T. M. Powers, A. R. Fout, S.-L. Zheng, T. A. Betley, *J. Am. Chem. Soc.* **2011**, *133*, 3336–3338; i) Q. Zhao, T. A. Betley, *Angew. Chem. Int. Ed.* **2011**, *50*, 709–712.

[13] a) M. Tachikawa, A. C. Sievert, E. L. Muetterties, M. R. Thompson, C. S. Day, V. W. Day, *J. Am. Chem. Soc.* **1980**, *102*, 1725–1727; b) L. H. Gade, *Angew. Chem. Int. Ed.* **2000**, *39*, 2658–2678.

[14] a) H.-C. Yu, J. Telser, N. P. Mankad, *Organometallics* **2021**, *40*, 2123–2132; b) Y. Lakliang, N. P. Mankad, *Organometallics* **2020**, *39*, 2043–2046; c) N. J. Leon, H.-C. Yu, T. J. Mazzacano, N. P. Mankad, *Polyhedron* **2019**, *157*, 116–123; d) N. P. Mankad, *Chem. Commun.* **2018**, *54*, 1291–1302; e) N. P. Mankad, *Chem. Eur. J.* **2016**, *22*, 5822–5829; f) K. T. Horak, S. Lin, J. Rittle, T. Agapie, *Organometallics* **2015**, *34*, 4429–4432; g) S. Banerjee, M. K. Karunananda, S. Bagherzadeh, U. Jayarathne, S. R. Parmelee, G. W. Waldhart, N. P. Mankad, *Inorg. Chem.* **2014**, *53*, 11307–11315; h) U. Jayarathne, T. J. Mazzacano, S. Bagherzadeh, N. P. Mankad, *Organometallics* **2013**, *32*, 3986–3992.

[15] a) F. A. Cotton, in *Metal Clusters in Chemistry*, (Eds.: P. Braunstein, L. A. Oro, P. R. Raithby), Wiley-VCH, Weinheim, **1999**, pp. 2–7; b) J. E. Ellis, *J. Am. Chem. Soc.* **1981**, *103*, 6106–6110.

[16] a) J. A. Kelly, J. Gramüller, R. M. Gschwind, R. Wolf, *Dalton Trans.* **2021**, *50*, 13985–13992; b) C. M. Hoidn, C. Rödl, M. L. McCrea-Hendrick, T. Block, R. Pöttgen, A. W. Ehlers, P. P. Power, R. Wolf, *J. Am. Chem. Soc.* **2018**, *140*, 13195–13199.

[17] a) J. E. Ellis, *Dalton Trans.* **2019**, *48*, 9538–9563; b) J. E. Ellis, *Inorg. Chem.* **2006**, *45*, 3167–3186; c) K. Jonas, C. Krüger, *Angew. Chem. Int. Ed.* **1980**, *19*, 520–537.

[18] W. W. Brennessel, J. E. Ellis, M. K. Pomije, V. J. Sussman, E. Urnezius, V. G. Young, *J. Am. Chem. Soc.* **2002**, *124*, 10258–10259.

[19] a) A. S. Romanov, C. R. Becker, C. E. James, D. Di, D. Credgington, M. Linnolahti, M. Bochmann, *Chem. Eur. J.* **2017**, *23*, 4625–4637; b) O. Santoro, A. Collado, A. M. Z. Slawin, S. P. Nolan, C. S. J. Cazin, *Chem. Commun.* **2013**, *49*, 10483–10485.

[20] a) A. Liske, K. Verlinden, H. Buhl, K. Schaper, C. Ganter, *Organometallics* **2013**, *32*, 5269–5272; b) R. H. Crabtree, *J. Organomet. Chem.* **2005**, *690*, 5451–5457; c) W. A. Herrmann, *Angew. Chem. Int. Ed.* **2002**, *41*, 1290–1309.

[21] a) V. J. Sussman, J. E. Ellis, *Angew. Chem. Int. Ed.* **2008**, *47*, 484–489; b) M. Jang, J. E. Ellis, *Angew. Chem. Int. Ed.* **1994**, *33*, 1973–1975; c) M. Y. Darensbourg, E. L. Muetterties, *J. Am. Chem. Soc.* **1978**, *100*, 7425–7428.

[22] Note that for the starting tantalate, **[Ta(naph)$_3$]$^-$**, NMR spectroscopic data are reported in THF-d_8. Data were collected for **1a** in this solvent, but for comparison to the other Ta/Cu species presented herein, the present chemical shifts are sourced from spectra collected in C_6D_6.

[23] Deposition numbers 2287351 (**1a**), 2287354 (**1b**), 2287355 (**1c**), 2287353 (**2b**), and 2287352 (**3a**) contain the supplementary crystallographic data for this paper. These data are provided free of charge by the joint Cambridge Crystallographic Data Centre and Fachinformationszentrum Karlsruhe Access Structures service.

[24] P. Pyykkö, M. Atsumi, *Chem. Eur. J.* **2009**, *15*, 186–197.

[25] T. M. Arkhireeva, B. M. Bulychev, A. I. Sizov, T. A. Sokolova, V. K. Belsky, G. L. Soloveichik, *Inorg. Chim. Acta* **1990**, *169*, 109–118.

[26] a) W.-Q. Zhang, H. W. T. Morgan, C.-C. Shu, J. E. McGrady, Z.-M. Sun, *Inorg. Chem.* **2022**, *61*, 4421–4427; b) R. Pätow, D. Fenske, *Z. Anorg. Allg. Chem.* **2002**, *628*, 2790–2794.

[27] M. Melaimi, R. Jazzar, M. Soleilhavoup, G. Bertrand, *Angew. Chem. Int. Ed.* **2017**, *56*, 10046–10068.

[28] For a related example of heteromultimetallic μ-arene C–H activation, see: S. Bajo, M. M. Alcaide, J. López-Serrano, J. Campos, *Chem. Eur. J.* **2021**, *27*, 16422–16428.

[29] Following addition of H_2, the ^{1}H NMR spectrum evidences the growth of a signal at 4.29 ppm (bound naphthyl proton). Additionally, there is no evidence for arene ligand exchange under these reaction conditions. See Supporting Information (Figures S40 and S41) for additional details.

[30] a) G. Zhu, K. E. Janak, J. S. Figueroa, G. Parkin, *J. Am. Chem. Soc.* **2006**, *128*, 5452–5461; b) E. P. Kündig, C. Perret, S. Spichiger, G. Bernardinelli, *J. Organomet. Chem.* **1985**, *286*, 183–200; c) E. L. Muetterties, J. R. Bleeke, A. C. Sievert, *J. Organomet. Chem.* **1979**, *178*, 197–216.

[31] W. A. G. Graham, *Inorg. Chem.* **1968**, *7*, 315–321.

[32] R. E. Jilek, M. Jang, E. D. Smolensky, J. D. Britton, J. E. Ellis, *Angew. Chem. Int. Ed.* **2008**, *47*, 8692–8695.

[33] a) Y. L. K. Tan, W. K. Leong, *J. Organomet. Chem.* **2007**, *692*, 768–773; b) R. D. Adams, T. S. Barnard, Z. Li, W. Wu, J. Yamamoto, *J. Am. Chem. Soc.* **1994**, *116*, 9103–9113.

[34] a) S. Grimme, J. Antony, S. Ehrlich, H. Krieg, *J. Chem. Phys.* **2010**, *132*, 154104; b) F. Weigend, R. Ahlrichs, *Phys. Chem. Chem. Phys.* **2005**, *7*, 3297–3305; c) C. Adamo, V. Barone, *J. Chem. Phys.* **1999**, *110*, 6158–6170; d) D. Andrae, U. Häußermann, M. Dolg, H. Stoll, H. Preuß, *Theor. Chim. Acta* **1990**, *77*, 123–141.

[35] K. B. Wiberg, *Tetrahedron* **1968**, *24*, 1083–1096.

[36] T. Lu, F. Chen, *J. Comput. Chem.* **2012**, *33*, 580–592.

[37] Similar analyses have been performed to interpret the electronic structure in related early-late heterobimetallic complexes. See: L. Rocchigiani, W. T. Klooster, S. J. Coles, D. L. Hughes, P. Hrobárik, M. Bochmann, *Chem. Eur. J.* **2020**, *26*, 8267–8280; and G. Jansen, M. Schubart, B. Findeis, L. H. Gade, I. J. Scowen, M. McPartlin, *J. Am. Chem. Soc.* **1998**, *120*, 7239–7251.

Manuscript received: August 11, 2023
Accepted manuscript online: October 13, 2023
Version of record online: October 27, 2023

© 2023 The Authors. Angewandte Chemie International Edition published by Wiley-VCH GmbH